

Quantitative Model to Forecast Changes in Hurricane Vulnerability of Regional Building Inventory

Rachel A. Davidson, A.M.ASCE¹; Huan Zhao²; and Vineet Kumar³

Abstract: This paper introduces a quantitative methodology to model the way the hurricane wind vulnerability of a region's building inventory changes over time due, for example, to aging, structural upgrading efforts, construction and demolition of buildings, and changing materials, construction technologies, and building code content and enforcement. The model aims to explore the overall rate of vulnerability change and the relative contributions of various societal and natural factors affecting it, and ultimately to be incorporated into regional risk assessment models. Current risk assessment models assume that a region's vulnerability remains constant over time. The methodology combines a component-based building vulnerability model, simulation, and Markov modeling. The vulnerability changes are represented by changes in the form of fragility curves over time. A limited scope sample analysis is presented for a model residential, wood-frame building category in North Carolina. The sample analysis addresses vulnerability changes due to building code changes only, and includes an investigation of the sensitivity of the results to several key parameters.

DOI: 10.1061/(ASCE)1076-0342(2003)9:2(55)

CE Database subject headings: Hurricanes; Wind loads; Damage assessment; Forecasting; North Carolina; Models.

Introduction

The vulnerability of a region's building stock to natural hazards continuously changes over time due, for example, to aging, structural upgrading efforts, construction and demolition of buildings, and changing materials, construction technologies, and building codes. In fact, many natural disaster risk management efforts rely on the assumption that we can affect this change such that vulnerability, and therefore risk, are reduced. Nevertheless, regional natural disaster risk assessment models (also known as loss estimation models) currently assume that building vulnerability remains constant through time. As a result, these models may incorrectly estimate risk. This paper introduces a methodology to model the way that the hurricane wind vulnerability of a region's building inventory changes over time. The model is being developed as part of a larger effort to model how hurricane risk changes over time. This paper focuses on the theoretical development of the vulnerability change methodology, which aims to be generic enough to allow inclusion of all causes of vulnerability change, and ultimately to be adapted to different hazards and regions. The paper's sample analysis, however, is restricted in scope, addressing only the hurricane wind hazard, vulnerability

changes due to building code changes, the time period from 2000 to 2020, and one residential, wood-frame building category in coastal North Carolina.

In this paper, vulnerability refers to the potential of the built environment to be damaged or destroyed. The vulnerability of a category of buildings (e.g., single-family wood-frame) is characterized by a set of fragility curves, each of which represents the probability that a building in that category will experience at least the associated damage state (e.g., minor, moderate, severe) given a certain wind speed. Changes in the vulnerability of a building category, therefore, are represented by changes in the form of the associated fragility curves (e.g., see Fig. 1). In loss estimation models, vulnerability models are combined in a Geographic Information System with a hazard model and structural inventory databases to estimate the expected loss in a region in a specified future time period (e.g., NIBS 2000, Rosowsky et al. 1999).

Many societal and natural factors affect the vulnerability of a region's building inventory. Some serve to increase it (e.g., aging); some to decrease it (e.g., improving building codes or their enforcement). A building vulnerability change model that explicitly simulates these effects can help shed light on which of these competing factors dominates and can show how their effects evolve over time.

A model that captures the way that building vulnerability changes over time can be incorporated into a loss estimation model to help create a methodology that models how a region's risk (i.e., expected annual losses) changes over time. Such a hurricane risk forecasting methodology can improve risk management decision support and risk communication in a few ways. First, since risk is changing, risk managers are chasing a moving target. Currently, planning for risk is often based on the way the world looks today. A hurricane risk forecasting model can help risk managers anticipate how the world will change, estimate what the losses will be at that time in the future when the next hurricane occurs, and plan for those future conditions. Second, when a risk management effort is made, the effects do not appear instantaneously. They are realized over time because there may be

¹Assistant Professor, School of Civil and Environmental Engineering, 373 Hollister Hall, Cornell Univ., Ithaca, NY 14853-3501. E-mail: rad24@cornell.edu

²Project Control Engineer, Bechtel Corporation, 5275 Westview Dr., Frederick, MD 21703. E-mail: hzhao@bechtel.com

³Graduate Student, School of Civil and Environmental Engineering, 220 Hollister Hall, Cornell Univ., Ithaca, NY 14853-3501. E-mail: vk52@cornell.edu

Note. Associate Editor: Samer M. Madanat. Discussion open until November 1, 2003. Separate discussions must be submitted for individual papers. To extend the closing date by one month, a written request must be filed with the ASCE Managing Editor. The manuscript for this paper was submitted for review and possible publication on March 19, 2002; approved on January 24, 2003. This paper is part of the *Journal of Infrastructure Systems*, Vol. 9, No. 2, June 1, 2003. ©ASCE, ISSN 1076-0342/2003/2-55-64/\$18.00.

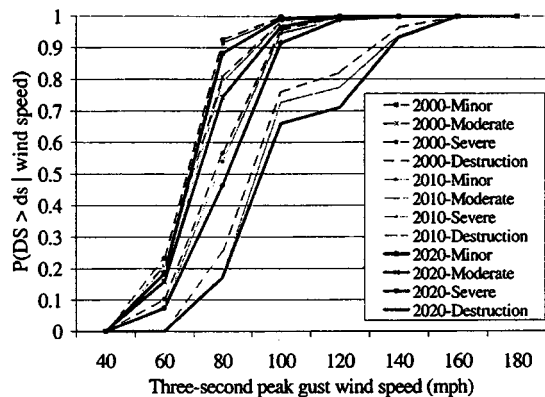


Fig. 1. Sample analysis results showing change in fragility curves over time

a delay between the decision and implementation, a delay in the policy having an effect on the risk (e.g., zoning laws actually reducing the number of structures in hazardous areas), or a delay in the time until the next hurricane occurs and the benefits of the effort are realized. A fully dynamic risk assessment model could show the user how the effects of his decisions will unfold over time. Third, by explicitly modeling the societal and natural factors effecting the change (e.g., demographic and building code changes), a hurricane risk forecasting methodology could allow assessment of the relative contributions of those factors. Understanding how these factors come together to create risk may suggest risk management opportunities that target the root causes of risk and can be most effective in the long term. Fourth, one of the reasons for a relatively low level of public concern about hurricane risk is that hurricanes are seen as part of the future, and therefore, as an issue that can be addressed at a later time. Risk forecasts can establish more directly and quantitatively the connection between today's actions and the effects of a hurricane 20 years from now (e.g., as a decision to build on the coast today creates inventory to be damaged in the next hurricane). A stronger connection between present and future can make hurricane risk more salient and encourage risk management activities.

This paper begins with a background on available vulnerability and vulnerability change models. The new building vulnerability change methodology is described in the next section. A sample application of the methodology is then presented, considering only the effects of building code changes for a model residential, wood-frame building category in North Carolina. The sample analysis is meant only to illustrate the model application and results, not to provide definitive conclusions about this study region. The paper concludes with summary remarks on the strengths and limitations of the methodology.

Background

Vulnerability Models

In applying vulnerability models, the built environment is divided into groups of structures that exhibit similar vulnerability. A separate vulnerability model (i.e., set of fragility curves) is developed for each group. A model building is typically defined within the building category, the vulnerability of the model building is analyzed, and it is assumed that its behavior represents that of all buildings in the category. There are two approaches to developing

a vulnerability model for a group of structures: (1) component-based and (2) direct. In the component-based approach, the vulnerability of the components of a structure (e.g., windows, roof) are each determined separately, and the vulnerability of the structure is determined based on the component vulnerabilities and their interactions. In the direct approach, the model is determined for the entire structure without considering components, for example, by deriving relationships between historical damage and wind speeds. Chiu (1994), Holmes (1996), Stubbs and Perry (1996), Unanwa et al. (2000), Unanwa and McDonald (2000), and NIBS (2000) offer examples of wind vulnerability models developed using the component-based approach. Examples of wind vulnerability models developed using the direct approach can be found in Leicester et al. (1979), Mitsuta et al. (1996), Sparks et al. (1994), and Rosowsky et al. (1999).

A building vulnerability change model requires a vulnerability model to serve as its foundation. The building vulnerability change model developed in this work is based on a simplified version of HAZUS, the NIBS (2000) model. Based on a draft technical manual, the HAZUS model will use a component-based approach that employs simulation to combine component damage into building damage. Discussions in the sections, "Overall Methodology" and "Component, Component State, and Damage State Definitions" explain specifically how the HAZUS methodology has been modified for use in this study. Although it is more calculation- and data-intensive than the direct approach, the component-based approach was selected because it allows more direct modeling of building code changes or other mitigation efforts than the direct approach. The simulation-based approach of HAZUS was chosen because it could be incorporated into the vulnerability change methodology and is publicly available.

Vulnerability Change Models

Currently, there are no available quantitative models of how the vulnerability of a region's building inventory to natural hazards changes over time. A recent report by the National Association of Home Builders (NAHB 2000) offers perhaps the best available macro-examination of building vulnerability change. The report, which is based on statistical data, construction documents, and personal interviews, describes the U.S. residential building inventory as a whole (not broken down regionally or otherwise) during three periods of time: the early-1900s, the mid-1900s, and the late-1900s. Stewart et al. (2000) uses the Rosowsky et al. (1999) direct vulnerability model to explore the effects of a few scenario-based hypothetical changes in vulnerability on estimated losses (e.g., if all houses were retrofit after experiencing hurricane damage, or if all new housing was constructed with reduced vulnerability). Tao et al. (1994) uses a Markov decision process-based modeling approach to identify an optimal design and maintenance policy for a specific structure. As part of the model, changes in a structure's resistance over time due to aging and maintenance efforts are simulated.

While those studies examine changes in building inventory from a broad perspective, studies of fastener corrosion and weathering and decay of wood (e.g., Browne 1960; Wilcox 1978; Bengelsdorf 1982) can be considered examinations of aging-related changes in building vulnerability at a microlevel. The building vulnerability change model introduced in the next section incorporates some of the findings of these macro- and micro-studies into a framework that explicitly, quantitatively models changes in a region's vulnerability over time.

Table 1. Sample Analysis Component and Building Damage States

Damage state	Damage description	Roof cover area failure	Window failure	Roof sheathing area failure	Roof-to-wall connection failure
0	No or very minor damage	$\leq 2.5\%$	None	None	No
1	Minor damage	$> 2.5\%$	≤ 2	None	No
2	Moderate damage	$\leq 15\%$	> 2	$\leq 5\%$	No
3	Severe damage	$> 15\%$	≤ 4	$> 5\%$	No
4	Destruction	$\leq 50\%$	> 4	$\leq 40\%$	No
		$> 50\%$	≤ 6	$> 40\%$	Yes

Note: A building is considered to be in the higher damage state if *any* of the italicized damage indicators in the corresponding row occurs. Based on NIBS (2000), as described in the section, "Component, Component State, and Damage State Definitions."

Building Vulnerability Change Model

Objectives and Scope

The building vulnerability change model aims to capture the way in which the vulnerability of a region's building inventory changes during each time step Δt in a specified time horizon T . The methodology was developed for residential construction and the hurricane wind hazard only, although it could be extended to include other structural types and hazards in the future. Vulnerability changes due to changes in the numbers, locations, or architectural styles of buildings are not included in this methodology, rather, they are addressed in a building inventory change model developed in conjunction with this model (Davidson and Rivera 2003).

Components

In this building vulnerability change model, each building is considered to be an assemblage of components, such as windows and roof sheathing. The expected performance of each component during a hurricane is evaluated separately, and together the components' damage determines the building's performance. Components included in the model are those that are key determinants of a building's damage level in hurricane winds. Those characteristics that depend on the building owner's style preferences are captured by the building inventory change model (e.g., number of stories, roof shape) (Davidson and Rivera 2003). Those that are more the result of structural performance considerations are captured in this vulnerability change model (e.g., roof covering attachment, roof-to-wall connection).

Each component type c has S_c possible states, defined as possible values of the mean component resistance. The actual resistance of a component in a given building is a random variable. At a point in time, for a given component, a state vector describes the probabilities of the component being in each state. The state vector is like a probability mass function for the mean component resistance. A Markov-based model is used to estimate how the state vector changes over time. The section, "Component, Component State, and Damage State Definitions" explains how component states are defined.

Overall Methodology

The building vulnerability change model uses simulation to determine, for each time step in the time horizon, a set of fragility curves for each component, and for a building as a whole. The

simulation, which is based on NIBS (2000), has seven basic steps. The simulation is done for one building category at a time. First, for each component c , the mean component resistance μ_{R_c} is randomly sampled from the probability mass function that describes the relative frequency of the component being in each state. Second, for each component, a value of the resistance of the component R_c is randomly sampled from a lognormal distribution with the specified mean resistance μ_{R_c} and coefficient of variation, CV_{R_c} . The lognormal distribution was chosen to keep the model simple while ensuring that the non-negativity constraint is fulfilled. Other distributions could easily be substituted for some or all components if evidence supported that decision. Component resistances are assumed to be independent. The variability modeled in Step 1 captures the fact that different buildings within a building category have different configurations for each component (e.g., for roof-to-wall connections, a building may use three $8d$ toe nails alone or three $8d$ toe nails plus a strap on every rafter). The variability in Step 2 recognizes that there is variability between buildings with the same component configuration (and even within one building) due to construction and material variability. Third, for each component, the component resistance R_c is compared to the wind load, I_{cw} , that would be applied to that component at each of a set of different three-second peak gust wind speeds w (40–200 mph). If the resistance is less than the load, the component fails at that wind speed; otherwise, it does not. The component wind loads I_{cw} resulting from each specified wind speed w are estimated deterministically as the design wind loads determined using ASCE 7-95 (ASCE 1995).

Fourth, the damage state of each component at each wind speed is determined using established damage state definitions. For example, if none of the roof sheathing fails, it has "no to minor damage;" if no more than 5% of the area of roof sheathing fails, it is in the "moderate damage" state; and so on. The roof sheathing is modeled as many discrete pieces, and the failure of each piece is modeled separately. The percentage of damage to roof sheathing, therefore, is based on the number of pieces of roof sheathing (and the associated percentage of roof area) that are damaged. The same approach holds for roof covering and windows. Fifth, the building damage state is determined based on the component damage states. For example, if no more than 2.5% of the roof covering fails, no windows fail, no roof sheathing fails, and the roof-to-wall connection does not fail, the building is in the "no or very minor damage" state (State 0). Table 1 shows the component and building damage states used in the sample analysis. Sixth, Steps 1 to 5 are repeated N (say, 1,000) times, and the frequency of each component and building damage state at each

wind speed within the N iterations are determined and used to develop fragility curves. Finally, for each component, the probability mass function of component states is updated using a Markov model (see next section) for the next time step. This updating reflects changes that occur in the mean resistances of building components. The entire process is repeated for each time step in the time horizon.

The component- and simulation-based vulnerability model that is the foundation of this methodology is similar to that used in HAZUS with a few significant simplifications. According to the draft technical manual (NIBS 2000), HAZUS reevaluates wind speed and direction at 15-min time intervals, allowing it to incorporate the effect of internal pressurization and to model the evolution of damage during a hurricane explicitly. At each time step, HAZUS calculates the wind loads on components l_{cw} using directionality-dependent pressure coefficients, rather than ASCE 7-95 design wind loads used in the simplified model in this study. HAZUS also accounts for the shielding effect of the terrain near a structure and computes the probability of a missile impact on a wall at each time step; the model in this paper does not. These simplifications were made to facilitate development of the vulnerability *change* model that is the focus of this research (and is not part of HAZUS) but if desired, it should be possible to incorporate the full HAZUS model when it is complete.

Markov-Based Model

For each component c , a methodology based on a stationary Markov chain is used to model the way that the component resistance changes over time. The S_c states of the Markov chain correspond to the possible values of mean resistance of the component μ_{Rc} . The variable $\pi_{ci}(t)$ represents the probability that the component is in state i at time t . The values of $\pi_{ci}(t)$ are all stored in a 1 by S_c state vector $\pi_c(t)$, which defines a probability mass function for the mean resistance of component c . An analogous methodology could be developed to model changes in the variance of component resistances, but at this time the coefficient of variation of the resistance CV_{Rc} is assumed to be constant over time for all components.

Changes in building vulnerability may occur due to one of four factors: (1) changes in the content of building codes B ; (2) changes due to technological innovations (e.g., introduction of a new material) or other societal factors T ; (3) structural aging A ; and (4) building upgrades U . During a given time step, the first two factors (B and T) affect only the vulnerability of new buildings that are constructed during that time step; the second two factors (A and U) affect only buildings that already existed at the beginning of the time step. The probability that component c of an existing building is in state i at time t , $\pi_{ci}^{EB}(t)$, is calculated using Eq. (1)

$$\pi_{ci}^{EB}(t) = \frac{\pi_{ci}^{EB}(t-1)EB_{t-1} + \pi_{ci}^{B,T}(t)e_tNB_t + \pi_{ci}^T(t)(1-e_t)NB_t - \pi_{ci}^{DB}(t)DB_t}{EB_t} \quad (1)$$

where EB_t = number of buildings that exist at time t ; NB_t and DB_t = number of new buildings built and buildings demolished between times $t-1$ and t , respectively; $\pi_{ci}^{B,T}(t)$ = probability that component c of a new building built to code between times $t-1$ and t is in state i ; $\pi_{ci}^T(t)$ = probability that component c of a new building not built to code, but built to the technology of the time between times $t-1$ and t is in state i ; $\pi_{ci}^{DB}(t)$ = probability that component c of a building demolished between time $t-1$ and t is in state i ; and e_t = percentage of new buildings built between times $t-1$ and t that are built to the current building code (i.e., for which the code is enforced). The first term in the numerator represents the number of buildings for which component c is in state i at $t-1$. The remaining terms represent the number of buildings built to code, the number of buildings built but not to code, and the number of buildings demolished between times $t-1$ and t for which component c is in state i . Dividing the numerator (i.e., the total number of buildings at time t for which component c is in state i) by the total number of buildings at time t gives the probability that a building at time t has component c in state i .

If it is assumed that the distribution of buildings demolished between $t-1$ and t is the same as that of buildings existing in time $t-1$, then $\pi_{ci}^{DB}(t) = \pi_{ci}^{EB}(t-1)$. Let n and d be the numbers of new buildings built and existing buildings demolished between times $t-1$ and t , expressed as percentages of the number of existing buildings at time $t-1$, EB_{t-1} . Substituting $NB_t = nEB_{t-1}$, $DB_t = dEB_{t-1}$, and $EB_t = EB_{t-1} + NB_t - DB_t$ and simplifying Eq. (1) yields Eq. (2)

$$\pi_{ci}^{EB}(t) = \frac{\pi_{ci}^{EB}(t-1) + \pi_{ci}^{B,T}(t)e_tn + \pi_{ci}^T(t)(1-e_t)n - \pi_{ci}^{EB}(t-1)d}{1+n-d} \quad (2)$$

The distribution of component mean resistances in buildings that existed in time $t-1$ may change during the time step due to the effects of aging or building owners undertaking structural upgrades. To represent those changes, the distribution of existing buildings is updated by a transition probability matrix, $P_c^{A,U}$. The distribution of component mean resistances in new buildings built to the current code and with current technology can be determined using a Markov chain: $\pi_c^{B,T}(t) = \pi_c^{B,T}(0)[P_c^{B,T}]^t$, where $\pi_c^{B,T}(0)$ is the initial state vector containing the probabilities that the code and current technology require component c to be in state i , and $P_c^{B,T}$ is a transition probability matrix representing changes in the content of the code and changes in technology. Similarly, the distribution of component mean resistances in new buildings built not to the current code but with current technology can be determined using a Markov chain: $\pi_c^T(t) = \pi_c^T(0)[P_c^T]^t$, where $\pi_c^T(0)$ is the initial state vector containing the probabilities that current technology require component c to be in state i , and P_c^T is a transition probability matrix representing changes in technology. Incorporating these elements into Eq. (2), and expanding each probability into a vector produces Eq. (3), which is used to update the probability mass function of component resistances in step 7 of the simulation

$$\pi_c^{EB}(t) = \frac{\pi_c^{EB}(t-1)[P_c^{A,U}] + \pi_c^{B,T}(0)[P_c^{B,T}]^t e_t n + \pi_c^T(0)[P_c^T](1-e_t)n - \pi_c^{EB}(t-1)d}{1+n-d} \quad (3)$$

Each value, $P_{cij}^{A,U}$ ($i, j = 1, 2, \dots, S_c$), in the $P_c^{A,U}$ matrix is defined as the probability of component c transitioning from state i to state j in one time step *due only to the effects of aging and upgrading*. The matrix $P_c^{A,U}$ is defined as a combination of two probability matrices P_c^A and P_c^U , which represent state changes due to aging only and due to upgrading only, respectively. The values in the two matrices are assessed, then the overall probability of a component's mean resistance changing from state i to j can be calculated using Eq. (4). The transition probability matrix $P_c^{B,T}$ is calculated similarly.

$$P_{cij}^{A,U} = \sum_k P_{cik}^A P_{ckj}^U \quad (4)$$

To implement this Markov-based model for a building category, the matrix states have to be defined; the new construction, demolition, and code enforcement rates, n , d , and e_t , respectively, have to be estimated; and probability values for the matrices (P_c^B , P_c^T , P_c^A and P_c^U) and the state vectors, $\pi_c^{EB}(0)$, $\pi_c^{B,T}(0)$, and $\pi_c^T(0)$ have to be estimated for each of the components. The section, "Parameter Estimation" describes how these parameters were estimated in the sample analysis.

Sample Analysis

To illustrate the application of the building vulnerability change model, a sample analysis was conducted for a model residential, wood-frame building category in coastal North Carolina, for the period 2000 to 2020 ($T=20$ years) with a five-year time step ($\Delta t=5$ years). Only the effects of building code changes are included in this sample analysis; aging, upgrading, and new technologies were not considered. The sample building category is described first. The following section discusses how the components, component states, and damage states were defined. Parameter estimation for the sample analysis is then discussed, and finally, the sample analysis results and sensitivity analysis are presented. The model has not been extensively calibrated, so this sample analysis is intended only to illustrate the application of the methodology and interpretation of the results.

Building Category Description

The building vulnerability change methodology should be applied to one building category at a time. One approach in developing vulnerability models is to define one or a few model buildings within the building category, analyze the vulnerability of the model building(s), and assume that its behavior represents that of all buildings in the category (e.g., NIBS 2000, Unanwa et al. 2000). In the sample analysis, a single model building is defined. It is a one-story, residential wood-frame building in coastal North Carolina. The applicable code for this type of building is the "North Carolina State Building Code, Volume for Residential" (NCBCC 1996). It has a 28 ft \times 40 ft rectangular floor plan, 9 ft walls, two 2.5 ft \times 4 ft sheet plate glass windows on each exterior wall, and a gable roof with a 1:2 slope. The roof sheathing is comprised of 4 ft \times 8 ft, 3/8 in. thick plywood panels and the roof covering is 1 ft \times 3 ft, 3-tab asphalt shingles. Nails used to attach

the roof covering are assumed to penetrate through the sheathing panels. Rafters are spaced 2 ft on center, and the eave width is 1 ft with soffit. The building is in a suburban or urban area (category B exposure in ASCE 7-95), and in the high-wind area as designated by the 1996 NC building code.

Building categories should be defined narrowly enough that the buildings within a category all exhibit sufficiently similar behavior, but broadly enough that there are not too many categories to efficiently apply the methodology to all the buildings in a region. A category definition will determine the applicable building code, the key building components, the number and size of each of those components, and the wind loads they experience. To the extent that other wood-frame, residential buildings in North Carolina have similar configurations that would result in similar wind loads on components, the sample analysis can be considered to apply to that larger building category. Additional work is necessary to define a complete set of appropriate building categories to which the methodology should be applied.

Component, Component State, and Damage State Definitions

For simplicity, only four key components were considered in the sample analysis: (1) roof covering attachment, $c=1$ (i.e., nailing schedule); (2) roof sheathing attachment, $c=2$ (i.e., nailing schedule); (3) roof-to-wall connection type, $c=3$ (e.g., toe nailed, strapped); and (4) window glass thickness $c=4$. Each section of roof and each window is considered to be a separate component. A typical building, therefore, has many roof covering and roof sheathing attachment components, and many window components. In the sample analysis, there are 44 roof sheathing components—36 the size of a full sheathing panel, and 8 half the size of a sheathing panel. Each full sheathing panel constitutes about 2.5% of the entire roof area. There are the equivalent of 14, 20, and 6 full roof sheathing components in ASCE 7-95 wind load zones 1, 2, and 3, respectively. Panels crossing two zones are considered to be in the zone with a higher load, and the capacities of the 44 sheathing panels are assumed to be independent of each other in the analysis. Zhao (2002) shows the roof component layout. Roof covering components are considered to have the same size and layout as the roof sheathing components. HAZUS (NIBS 2000) includes the same four components, plus doors and walls, which were not included in this sample analysis for simplicity.

Each component type has four or five possible states, defined as possible values of the mean component resistance. The number of states was selected so that there would be enough to adequately represent the variability in component states, but no more than necessary. In defining component states, it is necessary to determine a range of component resistances that covers all those that exist today or are likely to exist during the time horizon. For each component, therefore, based on past and current building codes, and on experimental evidence and analytical models in the literature, typical configurations are identified, and the mean resistance associated with each configuration is estimated. For example, typical roof sheathing attachment configurations identified are: (1) 6d nails at 12 in. on center (o.c.) on the edges and 12 in. o.c. on

Table 2. Roof Covering Component States and Values of P_1^B , $\pi_1^B(0)$, and $\pi_1^{EB}(0)$

P_1^B	State 0, 20 psf	State 1, 30 psf	State 2, 40 psf	State 3, 60 psf	State 4, 80 psf	Configurations
State 0 (20 psf) ^a	0	0	1	0	0	2, 12 g ^b
State 1 (30 psf)	0	0	1	0	0	3, 12 g
State 2 (40 psf)	0	0	0.75	0.25	0	4, 12 g
State 3 (60 psf)	0	0	0	0.5	0.5	6, 12 g
State 4 (80 psf)	0	0	0	0.25	0.75	8, 12 g
$\pi_1^{B,T}(0)$	0	0	1	0	0	
$\pi_1^{EB}(0)$	0.1	0.1	0.6	0.15	0.05	

Note: Configurations, $\pi_1^{B,T}(0)$, $\pi_1^{EB}(0)$, and P_1^B are based on building codes (NCBCC 1996, 1985, 1976, 1968; ICC 2000) and construction handbooks (Anderson 1992). Estimation of all values in this table is explained in more detail in Zhao (2002, 41–45).

^aMean component resistances were estimated by calculating nail withdrawal capacities based on the National Design Specification (NDS-97) for Wood Construction (AF&PA 1997).

^b x, y refers to using x nails of size y for each 3-tab, 1 ft×3 ft asphalt roof shingle strip.

the supports (12 in./12 in.), (2) 6d nails, 6 in./12 in., (3) 8d nails, 6 in./12 in., and (4) 8d nails, 6 in./6 in. Based on the American Plywood Association test results for Douglas Fir-Larch (Cunningham 1993), the mean resistances associated with these configurations were estimated to be 22 psf, 44 psf, 104 psf, and 131 psf, respectively. These mean resistances are then defined as the states. Thus, while all possible configurations of a component are not considered explicitly in defining component states, any configuration can be represented by the state with a similar mean resistance. Tables 2–5 show the states and associated configurations for the four components. Zhao (2002) provides details of how the component states were identified and the mean resistances were estimated for each component. Table 1 presents the component and building damage states defined for the sample analysis. A building is considered to be in the higher-damage state if any of the italicized damage indicators in the corresponding row occurs. Table 1 is similar to that used in HAZUS (NIBS 2000), but without columns for *wall structure failure, or missile impacts on walls*; with *window failure* replacing *window and door failure*; and with a few values adjusted slightly. The values were adjusted to fit the characteristics of the model building. For example, $\leq 2.5\%$ was used to define “no or very minor roof covering damage” rather than the $< 2\%$ used in HAZUS, because 2.5% corresponds to one 4 ft×8 ft panel, the unit used in the roof analysis. While it would be useful if Table 1 were the same as that in HAZUS to facilitate comparison, since the focus of this study was on the methodology development and since the HAZUS model is not finalized, it was not critical to use the identical damage state definitions at this time.

Parameter Estimation

The effects of aging, upgrading, and new technologies were not considered in the sample analysis [i.e., it was assumed that $P_c^A = P_c^U = P_c^T = I$ for all c ; and that $\pi_c^{B,T}(0) = \pi_c^B(0)$]. It was also assumed that buildings built between $t-1$ and t , but not to code, have the same distribution of states as those existing at time $t-1$ [i.e., $\pi_c^T(t) = \pi_c^{EB}(t-1)$]. A ten-year demolition rate of 15% was estimated using 1980 and 1990 Census data. Based on the census-based projections of buildings in 2000 to 2020 in Davidson and Rivera (2003), the ten-year construction rate was estimated as 20%. Based on those ten-year values, the five-year construction and demolition rates for the sample analysis were assumed to be $n=9.5\%$ and $d=7.8\%$, respectively [e.g., $(1 + n_{\text{ten-year}}) = (1 + n_{\text{five-year}})^2$]. It was assumed that the enforcement rate is 50% in 2000, and will increase by 10% every five years (making it 73% in 2020). Although little information on enforcement rates is available, these values are reasonable compared to evaluations of the Insurance Services Office, Inc. Building Code Effectiveness Grading Schedule for North Carolina (ISO 2002).

Based on an examination of changes in the North Carolina Residential Building Code from 1968 to the present (NCBCC 1968, 1976, 1985, 1996), possible future code changes were estimated for each component. Those possible future changes in the written code were then translated into probabilities of change in component resistances, the values in the code content transition matrices P_c^B (Zhao 2002). The past codes were also used to estimate the initial state vectors $\pi_c^{EB}(0)$ and $\pi_c^B(0)$.

Table 3. Roof Sheathing Component States and Values of P_2^B , $\pi_2^B(0)$, and $\pi_2^{EB}(0)$

P_2^B	State 0, 22 psf	State 1, 44 psf	State 2, 104 psf	State 3, 131 psf	Configurations
State 0 (22 psf) ^a	0	1	0	0	6d, 12 in./12 in. ^b
State 1 (44 psf)	0	0.5	0.5	0	6d, 6 in./12 in.
State 2 (104 psf)	0	0	0.75	0.25	8d, 6 in./12 in.
State 3 (131 psf)	0	0	0.5	0.5	8d, 6 in./6 in.
$\pi_2^{B,T}(0)$	0	1	0	0	
$\pi_2^{EB}(0)$	0.1	0.4	0.4	0.1	

Note: Configurations, $\pi_2^{B,T}(0)$, $\pi_2^{EB}(0)$, and P_2^B are based on building codes (NCBCC 1996, 1985, 1976, 1968; ICC 2000) and Cunningham (1993). Estimation of all values in this table is explained in Zhao (2002, 45–48).

^aMean component resistances were estimated based on APA test results (Cunningham 1993).

^b $x, y_1/y_2$ refers to using nails of size x at a distance of y_1 on center on the edges and y_2 on center on the supports.

Table 4. Roof-to-Wall Connection Component States and Values of P_3^B , $\pi_3^B(0)$, and $\pi_3^{EB}(0)$

P_3^B	State 0, 430 psf	State 1, 670 psf	State 2, 1,210 psf	State 3, 1,590 psf	State 4, 2,010 psf	Configurations
State 0 (430 psf) ^a	0.5	0	0.5	0	0	3, 8d, no strap ^b
State 1 (670 psf)	0	0.25	0.5	0.25	0	3, 16d, no strap
State 2 (1,210 psf)	0	0	0.5	0.5	0	3, 8d, 1 small strap every other rafter
State 3 (1,590 psf)	0	0	0.25	0.65	0.1	3, 8d, 1 small strap every rafter
State 4 (2,010 psf)	0	0	0	0.75	0.25	3, 8d, 2 small straps every rafter
$\pi_3^{B,T}(0)$	0	0	0	1	0	
$\pi_3^{EB}(0)$	0.5	0.09	0.2	0.2	0.01	

Note: Configurations, $\pi_1^{B,T}(0)$, $\pi_1^{EB}(0)$, and P_1^B are based on building codes (NCBCC 1996, 1985, 1976, 1968; ICC 2000). Estimation of all values in this table is explained in more detail in Zhao (2002, 48–51).

^aMean component resistances estimated based on test results from Conner et al. (1987) and Reed et al. (1997).

^bx, y, z refers to using x nails of size y for toe-nailing and straps as described in z.

Consider the roof sheathing attachment component, for example. The 1968 through 1985 North Carolina codes simply require that “all roof sheathing shall be securely nailed to rafters at each bearing” (NCBCC 1976, 25). In the 1996 NC code, nail size and spacing are specified for different panel thicknesses. For panels with thickness from 5/16 to 1/2 in., the code requires use of 6d nails at 6 in./12 in. spacing. For panels with thicknesses from 19/32 to 3/4 in. it requires use of 8d nails at 6 in./12 in. In the 2000 international residential code, which North Carolina is expected to adopt, the requirement for 5/16 to 1/2 in. thick panels is upgraded to require use of 8d nails (ICC 2000). No particular specification is given for high-wind treatment in any of the code versions. The American Plywood Association recommends closer nail spacing for high wind regions (Cunningham 1993). For example, with 8d nails, it recommends 6 in./6 in. spacing. Based on these changes in the roof sheathing attachment code requirements over the past 30 years, the distribution of configurations in the building inventory in 2000 $\pi_c^{EB}(0)$, the code requirements in 2000 $\pi_c^B(0)$, and the probabilities that the content of the building code will change from one configuration to another in a given five-year period P_{cij}^B , were estimated (Table 3). It was estimated, for example, that if the code required 8d nails, 6 in./12 in., then in the next five years there would be a 75% chance that it would stay the same and a 25% that it would change to a requirement of 8d nails, 6 in./12 in. (Table 3). Conducting similar analyses for each component yielded the component states and parameter values in Tables 2–5. Zhao (2002) explains in detail the identification of component states and estimation of parameter values for all components.

For roof covering, note that since the initial state of the building code content is State 2 and the probability of transitioning from States 2, 3, or 4 to States 0 or 1 is zero, there is no way that

the code content will enter States 0 or 1. Therefore, the values in the first two rows of the code content transition matrix P_1^B do not matter, and they are defined to be [0 0 1 0 0]. States 0 and 1 are nonetheless included in the matrix because some of the existing buildings are in those states. A similar situation exists for the roof sheathing component.

Sample Analysis Results

For each component, the probability of being in each damage state at each time step was calculated by applying the Markov model procedure, using the parameter values given in the section, “Parameter Estimation” (Table 6). Table 6 shows, for example, that the probability that a building’s roof sheathing attachment is in State 2 (i.e., has a mean resistance of 104 psf) is 0.40 in year 2000, 0.42 in 2010, and 0.44 in 2020. The increasing resistance over time is a result of the analysis that the building code will continue to require more resistance over time.

Using the simulation procedure to combine the Markov model results with the damage definition matrix, resulted in a set of fragility curves for each time step (2000, 2005, 2010, 2015, and 2020), for the building overall and for each of the components. As an example, Fig. 1 shows how the model suggests that overall building fragility curves will change over time from 2000 to 2010 to 2020. In Fig. 1, the fragility curves move to the right as time goes on, indicating the building becomes less vulnerable. This is expected because the sample analysis only takes into account changes in building code content, which would serve to reduce vulnerability. Specifically, Fig. 1 shows, for example, that at 80 mph (Category 1 hurricane), the probability of having at least moderate damage is 0.81 in 2000, 0.79 in 2010, and 0.74 in 2020. By incorporating this information into a larger hurricane risk fore-

Table 5. Window Component States and Values of P_4^B , $\pi_4^B(0)$, and $\pi_4^{EB}(0)$

P_4^B	State 0, 50 psf	State 1, 60 psf	State 2, 70 psf	State 3, 100 psf	Configurations
State 0 (50 psf) ^a	0.5	0.5	0	0	3/16 in. sheet ^b
State 1 (60 psf)	0	0.75	0.25	0	7/32 in. sheet
State 2 (70 psf)	0	0	0.9	0.1	1/4 in. sheet
State 3 (100 psf)	0	0	0	1	5/16 in. sheet
$\pi_4^{B,T}(0)$	1	0	0	0	
$\pi_4^{EB}(0)$	0.5	0.3	0.15	0.05	

Note: Configurations, $\pi_1^{B,T}(0)$, $\pi_1^{EB}(0)$, and P_1^B are based on building codes (NCBCC 1996, 1985, 1976, 1968; ICC 2000). Estimation of all values in this table is explained in more detail in Zhao (2002, 51–53).

^aMean component resistances were estimated based on Fig. R-208.5 in NCBCC (1996).

^bRefers to thickness of plate glass windows.

Table 6. Component State Probabilities, $\pi_c^{EB}(t)$, for Years 2000, 2010, and 2020

Time	State	Roof covering	Roof sheathing	Roof-to-wall connection	Windows
2000	0	0.10	0.10	0.50	0.50
	1	0.10	0.40	0.09	0.30
	2	0.60	0.40	0.20	0.15
	3	0.15	0.10	0.20	0.05
	4	0.05	—	0.01	—
2010	0	0.09	0.09	0.45	0.49
	1	0.09	0.40	0.08	0.33
	2	0.60	0.42	0.21	0.14
	3	0.16	0.10	0.24	0.05
	4	0.05	—	0.02	—
2020	0	0.08	0.08	0.40	0.44
	1	0.08	0.36	0.07	0.35
	2	0.58	0.44	0.22	0.16
	3	0.18	0.11	0.28	0.04
	4	0.08	—	0.03	—

casting methodology, one could estimate quantitatively, the changes in expected losses due to hurricanes over time that are due to changes in building vulnerability.

If each damage state is related to an expected damage ratio (repair cost/replacement value), then the changes in vulnerability can be examined in terms of the expected dollar losses that would be avoided as a result. As a simple example, suppose that the damage ratios associated with no, minor, moderate, severe damage, and destruction are 0, 5, 20, 50, and 100%, respectively. The expected damage ratio given 80 mph wind speed then would be 41.6, 36.7, and 32.4%, in 2000, 2010, and 2020, respectively. For a \$100,000 building, that would translate into expected losses, given 80 mph winds, of \$41,600, \$36,700, and \$32,400 in 2000, 2010, and 2020, respectively. The reduction in vulnerability from 2000 to 2020 would save \$9,200, given 80 mph winds. Incorporating the relative probabilities of each wind speed would allow calculation of an overall expected loss for each year.

Sensitivity Analysis

A sensitivity analysis was conducted to assess the effects of five key parameters on the final resulting fragility curves: e_t , n , d , $\pi_c^{EB}(0)$, and P_c^B . Thirteen scenarios were considered in addition

to the base case (Table 7). In each scenario, only one parameter was changed, while the others remained at their base case values. Little or no information was available on probability distributions for the parameter values, so the investigators made subjective assessments of what they considered to be reasonable high and low estimates of each. For $\pi_c^{EB}(0)$ and P_c^B , an optimistic and pessimistic estimate was made for each component (optimistic corresponds to reduced vulnerability). For e_t , n , and d , three possible values of each were considered (Table 7). While these rough estimations do not allow precise comparison of the relative influence of the five parameters, they do enable an approximate exploration of the sensitivity of the results to parameter values.

According to the sensitivity analysis, varying the existing building initial state vectors $\pi_c^{EB}(0)$ had the greatest impact on the fragility curves. The maximum effect was to cause a change in the probability of experiencing at least moderate damage (State 2) from 0.46 to 0.58. Across all damage states and wind speeds in Scenarios 3 and 4, the average absolute value of the change in the probability of experiencing at least a specified damage state was 0.036. The significant effect of the $\pi_c^{EB}(0)$ vectors seems reasonable since they determine the vulnerability of the initial distribution of buildings as well as which buildings will be demolished.

The rate of new construction n and the enforcement rate e_t were the next most influential parameters. Across Scenarios 8–10, the average probability change was 0.026; across Scenarios 5–7, the average probability change was 0.023. The fragility curves were probably less sensitive to these parameters than $\pi_c^{EB}(0)$, even though the range of e_t values was very large, because they influence only new buildings. The parameters n and e_t interact so that the effect of e_t increases with the value of n , and vice versa. Intuitively, the extent to which the building code is enforced in new construction only makes a difference if new buildings are built; and conversely, the amount of new construction can reduce a region's vulnerability only if the building code is enforced in that new construction. The fragility curves were least sensitive to the building code change matrices P_c^B and the demolition rate d . Across Scenarios 1–2, the average probability change was 0.013; across Scenarios 11–13, the average probability change was 0.003. The P_c^B matrices were probably not very influential because they affect only a relatively small proportion of the building inventory, those buildings that are newly built to code. The effect of the demolition rate was limited by the assumption that the distribution of buildings that are demolished is the same as the distribution of existing buildings. The rate of new

Table 7. Sensitivity Analysis Scenario Definitions

Value of changed parameter	Value of changed parameter	Value of changed parameter
1 P_c^B are all adjusted to be optimistic, e.g., $P_4^B = \begin{bmatrix} 0.4 & 0.4 & 0.15 & 0.05 \\ 0 & 0.6 & 0.3 & 0.1 \\ 0 & 0 & 0.85 & 0.15 \\ 0 & 0 & 0 & 1 \end{bmatrix}$	3 $\pi_c^{EB}(0)$ adjusted to be optimistic: $\pi_1^{EB}(0) = [0.05 \ 0.05 \ 0.6 \ 0.2 \ 0.1]$ $\pi_2^{EB}(0) = [0.05 \ 0.3 \ 0.5 \ 0.15]$ $\pi_3^{EB}(0) = [0.45 \ 0.05 \ 0.2 \ 0.25 \ 0.05]$ $\pi_4^{EB}(0) = [0.45 \ 0.25 \ 0.2 \ 0.1]$	5 $e_{2000} = 100\%$, rate of growth = 0%/5 years 6 $e_{2000} = 75\%$, rate of growth = 5%/5 years 7 $e_{2000} = 0\%$, rate of growth = 0%/5 years
2 P_c^B are all adjusted to be pessimistic, e.g., $P_4^B = \begin{bmatrix} 0.75 & 0.25 & 0 & 0 \\ 0 & 0.95 & 0.05 & 0 \\ 0 & 0 & 0.95 & 0.05 \\ 0 & 0 & 0 & 1 \end{bmatrix}$	4 $\pi_c^{EB}(0)$ adjusted to be pessimistic: $\pi_1^{EB}(0) = [0.15 \ 0.15 \ 0.6 \ 0.1 \ 0]$ $\pi_2^{EB}(0) = [0.15 \ 0.5 \ 0.3 \ 0.05]$ $\pi_3^{EB}(0) = [0.55 \ 0.14 \ 0.2 \ 0.1 \ 0.01]$ $\pi_4^{EB}(0) = [0.55 \ 0.35 \ 0.1 \ 0]$	8 $n = 5\%$ 9 $n = 20\%$ 10 $n = 30\%$ 11 $d = 3\%$ 12 $d = 15\%$ 13 $d = 30\%$

Note: The base case is $\pi_c^{EB}(0)$ and P_c^B values are in Tables 2–5, $e_{2000} = 50\%$, rate of growth of $e_1 = 10\%$ per 5 years, $n = 9.5\%$, $d = 7.8\%$.

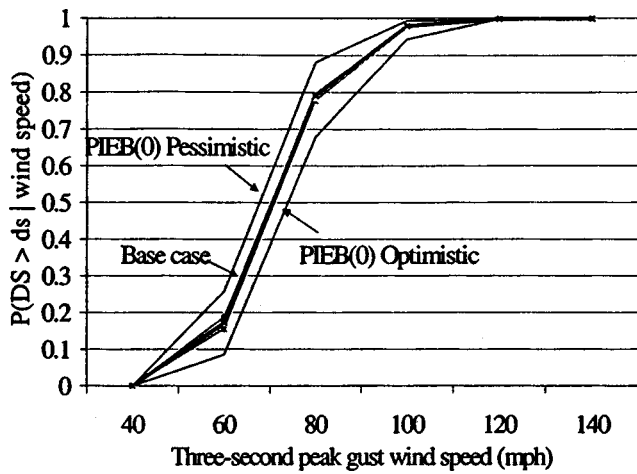


Fig. 2. Sensitivity analysis results for at least moderate damage in 2010

construction n was somewhat more influential than the rate of demolition d because all new buildings built to code are assumed to have reduced vulnerability, whereas not only the most vulnerable buildings are demolished.

The results of the sensitivity analysis can be shown graphically as well, by plotting the new fragility curves resulting from each scenario and comparing them with each other and with the base case. Given the parameter uncertainty assumed in the 13 scenarios, therefore, the sensitivity analysis enables the development of rough bounds on the fragility curves produced in the analysis. For example, Fig. 2 illustrates the range of realizations determined in the sensitivity analysis for one of the fragility curves (at least moderate damage in 2010). It shows how this particular fragility curve changed very little for all sensitivity analysis scenarios except the ones in which the $\pi_c^{EB}(0)$ vectors were altered. All of the 2010 fragility curves were similarly bounded by the scenarios in which $\pi_c^{EB}(0)$ were altered. In 2020, the outer bounds were either from the scenarios in which the $\pi_c^{EB}(0)$ vectors were altered, or from those in which n was altered.

In general, the estimated damage state probabilities at higher wind speeds (160 mph and higher) were not sensitive to parameter uncertainty because at those wind speeds, the probabilities of failure were all close to one. The analysis also suggests that the fragility curves for lower-damage states were more sensitive to parameter variation at lower wind speeds (e.g., 80 mph), and fragility curves for higher-damage states were more sensitive to parameter variation at higher wind speeds (e.g., 120 mph). As expected, the estimated damage state probabilities were most sensitive at the end of the time horizon 2020 because they were subject to the cumulative effect of the uncertainty in parameters in each previous time step.

Conclusions

The building vulnerability change model presented offers a new, quantitative way to study the evolution of a region's building vulnerability to hurricane winds over time. When integrated into a regional wind loss estimation model, it may be used to examine the way that hurricane-related losses change over time, thus improving regional loss estimations and the risk management decisions that rely on them. While the methodology currently focuses

on residential buildings and the hurricane wind hazard, it is generic enough that it may be expanded to address additional building categories and hazards.

Nevertheless, the methodology has several limitations at this time. As with any model, the results are only as good as the data used to obtain them. In this case, some of the required data are hard to find or require difficult subjective assessments. The sample analysis suggests, however, that it is possible to obtain estimates that are adequate for drawing general conclusions about the trends in regional vulnerability over time and for exploring the relative effects of various parameters on those trends. Additional work is necessary to define appropriate building categories to which the methodology should be applied. The model also should be calibrated with observed damage data before its results are used to support decisionmaking. Use of the methodology to model vulnerability changes due to structural aging, technological changes, and upgrading have not yet been demonstrated. Those forces of change, which could be more important than building codes, may involve additional complications when being incorporated into an analysis for a region. These are topics for future work.

Acknowledgments

The writers would like to thank the Cornell University College of Engineering for supporting this work through the McMullen Fellowship, and David Rosowsky for his valuable input throughout the project.

Notation

The following symbols are used in this paper:

CV_{Rc} = coefficient of variation of resistance of component c ;

d = number of existing buildings demolished between times $t-1$ and t , as a percentage of number of existing buildings at time $t-1$;

DB_t = number of existing buildings demolished between times $t-1$ and t ;

EB_t = number of buildings existing at time t ;

e_t = percentage of new buildings built between times $t-1$ and t that are built to the current code;

l_{cw} = ASCE 7-95 design wind load on component c given three-second peak gust wind speed w ;

N = number of iterations in simulation;

NB_t = number of new buildings built between times $t-1$ and t ;

n = number of new buildings built between times $t-1$ and t , as a percentage of the number of existing buildings at time $t-1$;

P_c^A, P_{cij}^A = transition matrix due to aging only, and its element;

$P_c^{A,U}, P_{cij}^{A,U}$ = transition matrix due to aging and upgrading, and its element;

P_c^B, P_{cij}^B = transition matrix due to building code only, and its element;

$P_c^{B,T}, P_{cij}^{B,T}$ = transition matrix due to building code and technology changes, and its element;

P_c^T, P_{cij}^T = transition matrix due to technology changes only, and its element;
 P_c^U, P_{cij}^U = transition matrix due to upgrading only, and its element;
 R_c = resistance of component c ;
 S_c = number of possible states for component c ;
 T = time horizon;
 t = time;
 Δt = time step;
 μ_{Rc} = mean resistance of component c ;
 $\pi_{ci}^{B,T}(t)$ = probability that component c of new building built to code and with current technology between times $t-1$ and t is in state i ;
 $\pi_{ci}^{DB}(t)$ = probability that component c of building that is demolished between times $t-1$ and t is in state i ;
 $\pi_{ci}^{EB}(t)$ = probability that component c of an existing building is in state i at time t ; and
 $\pi_{ci}^T(t)$ = probability that component c of new building not built to code, but built with current technology between times $t-1$ and t is in state i .

References

- American Forest & Paper Association (AF&PA). (1997). *NDS, National design specification for wood construction*, Washington, D.C.
- American Society of Civil Engineers (ASCE). (1995). *Minimum design loads for buildings and other structures*, ASCE 7-95. New York.
- Anderson, L. O. (1992). *Wood-frame house construction*, Craftsman Book, Carlsbad, Calif.
- Bengelsdorf, M. F. (1982). "Fastener corrosion in waterborne-preservative-treated wood." *Structural use of wood in adverse environments*, R. W. Meyer and R. M. Kellogg, eds. Van Nostrand Reinhold, New York, 131–141.
- Browne, F. L. (1960). "Wood siding left to weather naturally." *The Southern Lumberman*, 201(2513), 141–143.
- Chiu, G. L. F. (1994). "An extreme-wind risk assessment system." PhD thesis, Dept. of Civil Engineering, Stanford Univ., Stanford, Calif.
- Conner, H. W., Gromala, D. S., and Burgess, D. W. (1987). "Roof connections in houses: Key to wind resistance." *J. Struct. Eng.*, 113(12), 2459–2474.
- Cunningham, T. P. (1993). "Roof sheathing fastening schedules for wind uplift." *American Plywood Association (APA) Rep. No. T92-28*, Tacoma, Wash.
- Davidson, R., and Rivera, M. (2003). "Projecting changes in the Carolina building inventory and their effect on hurricane risk." *J. Urban Plann. Dev. Div., Am. Soc. Civ. Eng.*, in press.
- Holmes, J. (1996). "Vulnerability curves for buildings in tropical-cyclone regions." *Proc., ASCE Probabilistic Mechanics and Structural Reliability Specialty Conference*, ASCE, Worcester, Mass., 78–81.
- Insurances Services Office, Inc. (ISO) mitigation online. (2002). (<http://www.isomitigation.com/index.html#>) (Jan. 14, 2002).
- International Code Council (ICC). (2000). *International residential code, For one- and two-family dwellings*. Falls Church, Va.
- Leicester, R. H., Bubbs, C. T. J., Dorman, C., and Beresford, F. D. (1979). "An assessment of potential cyclone damage to dwellings in Australia." *Proc., 5th Int. Conf. Wind Engineering*, Fort Collins, Colo.
- Mitsuta, Y., Fujii, R., and Nagashima, I. (1996). "A predicting method of typhoon wind damages." *Proc., ASCE Probabilistic Mechanics and Structural Reliability Specialty Conf.*, ASCE, Worcester, Mass., 970–973.
- National Association of Home Builders (NAHB). (2000). "A historical profile of structural materials and methods for home building in the United States: 1900–2000." *Draft Rep.* Upper Marlboro, Md.
- National Institute of Buildings Sciences (NIBS). (2000). "HAZUS wind loss estimation methodology." *Draft Technical Manual*, Washington, D.C.
- North Carolina Building Code Council (NCBCC). (1968). *North Carolina uniform residential building code*. Raleigh, N.C.
- North Carolina Building Code Council (NCBCC). (1976). *North Carolina uniform residential building code, 1968 Ed. with amendments 1969–1976*. Raleigh, N.C.
- North Carolina Building Code Council (NCBCC). (1985). *North Carolina uniform residential building code, 1968 Ed. with amendments through December 10, 1985*. Raleigh, N.C.
- North Carolina Building Code Council (NCBCC). (1996). *North Carolina state building code, vol. VII—Residential, 1993 Ed. with amendments through June 13, 1996*. Raleigh, N.C.
- Reed, T. D., Rosowsky, D. V., and Schiff, S. D. (1997). "Uplift capacity of light-frame rafter to top plate connections." *J. Architect. Eng.*, 3(4), 156–163.
- Rosowsky, D., Sparks, P., and Huang, Z. (1999). "Wind field modeling and hurricane hazard analysis." South Carolina Sea Grant Consortium and Civil Engineering Dept., Clemson Univ., Clemson, S.C.
- Sparks, P. R., Schiff, S. D., and Reinhold, T. A. (1994). "Wind damage to envelopes of houses and consequent insurance losses." *J. Wind. Eng. Ind. Aerodyn.*, 53, 145–155.
- Stewart, M. G., Rosowsky, D. V., and Huang, Z. (2000). "Hurricane damage risk-cost-benefit analysis and the economic viability of strengthening new and existing residential construction." *Wood Engineering and Mechanics Research and Rep. No. WEM-00-001*. Oregon State University, Corvallis, Ore.
- Stubbs, N., and Perry, D. C. (1996). "A damage simulation model for buildings and contents in a hurricane environment." *Proc., ASCE Structures Congress XIV*, ASCE, Chicago, 989–996.
- Tao, Z., Corotis, R. B., and Ellis, J. H. (1994). "Reliability-based bridge design and life cycle management with Markov design processes." *Struct. Safety*, 16(1–2), 111–132.
- Unanwa, C. O., and McDonald, J. R. (2000). "Building wind damage prediction and mitigation using damage bands." *Nat. Hazards Rev.*, 1(4), 197–203.
- Unanwa, C. O., McDonald, J. R., Mehta, K. C., and Smith, D. A. (2000). "The development of wind damage bands for buildings." *J. Wind. Eng. Ind. Aerodyn.*, 84, 119–149.
- Wilcox, W. W. (1978). "Review of literature on the effects of early stages of decay on wood strength." *Wood Fiber*, 9(4), 252–257.
- Zhao, H. (2002). "A quantitative model forecasting changes in the hurricane vulnerability of residential wood-frame structures in North Carolina." MS thesis, School of Civil and Environmental Engineers Cornell Univ., Ithaca, N.Y.